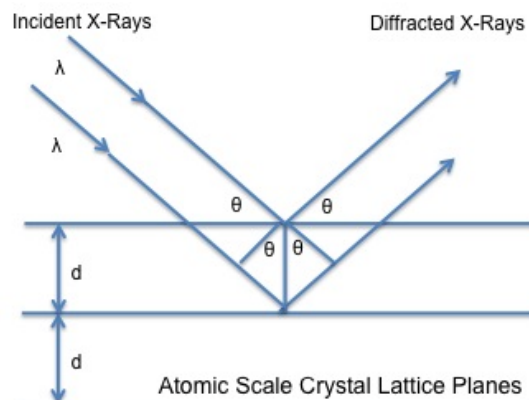


**Figure 6.89:** Australian-born British physicist William L. Bragg (1890 - 1971).

---

It has been used to determine the spacing of planes and angles formed between these planes and the incident beam that had been applied to the crystal examined. Intense scattered X-rays are produced when X-rays with a set wavelength are executed to a crystal. These scattered X-rays will interfere constructively due the equality in the differences between the travel path and the integral number of the wavelength. Since crystals have repeating units patterns, diffraction can be seen in terms of reflection from the planes of the crystals. The incident beam, the diffracted beam and normal plane to diffraction need to lie in the same geometric plane. The angle, which the incident beam forms when it hits the plane of the crystal, is called  $2\theta$ . Figure 6.90 shows a schematic representation of how the incident beam hits the plane of the crystal and is reflected at the same angle  $2\theta$ , which the incident beam hits. Bragg's Law is mathematically expressed, (6.17), where,  $n$ = integer order of reflection,  $\lambda$ = wavelength,  $d$ = plane spacing.



**Figure 6.90:** Bragg's Law construction.

$$n\lambda = 2d \sin\theta \quad (6.17)$$

Bragg's Law is essential in determining the structure of an unknown crystal. Usually the wavelength is known and the angle of the incident beam can be measured. Having these two known values, the plane spacing of the layer of atoms or ions can be obtained. All reflections collected can be used to determine the structure of the unknown crystal material.

Bragg's Law applies similarly to neutron diffraction. The same relationship is used the only difference being is that instead of using X-rays as the source, neutrons that are ejected and hit the crystal are being examined.

#### 6.4.1.2 Neutron diffraction

Neutrons have been studied for the determination of crystalline structures. The study of materials by neutron radiation has many advantages against the normally used such as X-rays and electrons. Neutrons are scattered by the nucleus of the atoms rather than X-rays, which are scattered by the electrons of the atoms. These generates several differences between them such as that scattering of X-rays highly depend on the atomic number of the atoms whereas neutrons depend on the properties of the nucleus. These lead to a greater and accurately identification of the unknown sample examined if neutron source is being used. The nucleus of every atom and even from isotopes of the same element is completely different. They all have different characteristics, which make neutron diffraction a great technique for identification of materials, which have similar elemental composition. In contrast, X-rays will not give an exact solution if similar characteristics are known between materials. Since the diffraction will be similar for adjacent atoms further analysis needs to be done in order to determine the structure of the unknown. Also, if the sample contains light elements such as hydrogen, it is almost impossible to determine the exact location of each of them just by X-ray diffraction or any other technique. Neutron diffraction can tell the number of light elements and the exact position of them present in the structure.

##### 6.4.1.2.1 Neutron inventors

Neutrons were first discovered by James Chadwick in 1932 Figure 6.91 when he showed that there were uncharged particles in the radiation he was using. These particles had a similar mass of the protons but did not have the same characteristics as them. Chadwick followed some of the predictions of Rutherford who

first worked in this unknown field. Later, Elsasser designed the first neutron diffraction in 1936 and the ones responsible for the actual constructing were Halban and Preiswerk. This was first constructed for powders but later Mitchell and Powers developed and demonstrated the single crystal system. All experiments realized in early years were developed using radium and beryllium sources. The neutron flux from these was not sufficient for the characterization of materials. Then, years passed and neutron reactors had to be constructed in order to increase the flux of neutrons to be able to realize a complete characterization the material being examined.

Between mid and late 40s neutron sources began to appear in countries such as Canada, UK and some other of Europe. Later in 1951 Shull and Wollan (Figure 6.87) presented a paper that discussed the scattering lengths of 60 elements and isotopes, which generated a broad opening of neutron diffraction for the structural information that can be obtained from neutron diffraction.



**Figure 6.91:** English Nobel laureate in physics James Chadwick (1891-1974)

---

### 6.4.2 Neutron sources

The first source of neutrons for early experiments was gathered from radium and beryllium sources. The problem with this, as already mentioned, was that the flux was not enough to perform huge experiments such as the determination of the structure of an unknown material. Nuclear reactors started to emerge in early 50s and these had a great impact in the scientific field. In the 1960s neutron reactors were constructed depending on the desired flux required for the production of neutron beams. In USA the first one constructed was the High Flux Beam Reactor (HFBR). Later, this was followed by one at Oak Ridge Laboratory (HFIR) (Figure 6.92), which also was intended for isotope production and a couple of years later the ILL was built. This last one is the most powerful so far and it was built by collaboration between Germany and France. These nuclear reactors greatly increased the flux and so far there has not been constructed any other better reactor. It has been discussed that probably the best solution to look for greater flux is to look for other approaches for the production of neutrons such as accelerator driven sources. These could greatly increase the flux of neutrons and in addition other possible experiments could be executed. The key point in these devices is spallation, which increases the number of neutrons executed from a single proton and the energy released

is minimal. Currently, there are several of these around the world but investigations continue searching for the best approach of the ejection of neutrons.

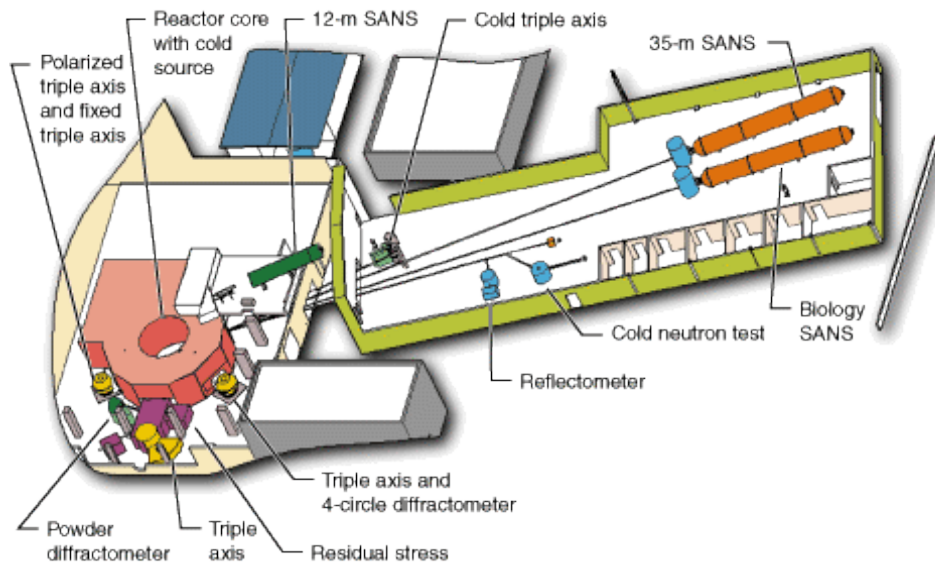
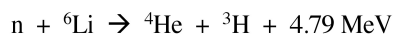
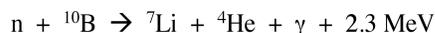
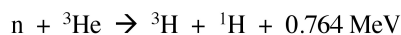


**Figure 6.92:** Schematic representation of HIFR. Courtesy of Oak Ridge National Laboratory, US Dept. of Energy

### 6.4.3 Neutron detectors

Although neutrons are great particles for determining complete structures of materials they have some disadvantages. These particles experiment a reasonably weak scattering when looking especially to soft materials. This is a huge concern because there can be problems associated with the scattering of the particles which can lead to a misunderstanding in the analysis of the structure of the material.

Neutrons are particles that have the ability to penetrate through the surface of the material being examined. This is primarily due to the nuclear interaction produced from the particles and the nucleus from the material. This interaction is much greater than the one performed from the electrons, which it is only an electrostatic interaction. Also, it cannot be omitted the interaction that occurs between the electrons and the magnetic moment of the neutrons. All of these interactions discussed are of great advantage for the determination of the structure since neutrons interacts with every single nucleus in the material. The problem comes when the material is being analyzed because neutrons being uncharged materials make them difficult to detect them. For this reason, neutrons need to be reacted in order to generate charged particles, ions. Some of the reactions usually used for the detection of neutrons are:



The first two reactions apply when the detection is performed in a gas environment whereas the third one is carried out in a solid. In each of these reaction there is a large cross section, which makes them ideal

for neutron capture. The neutron detection hugely depends on the velocity of the particles. As velocity increases, shorter wavelengths are produced and the less efficient the detection becomes. The particles that are executed to the material need to be as close as possible in order to have an accurate signal from the detector. These signal needs to be quickly transduced and the detector should be ready to take the next measurement.

In gas detectors the cylinder is filled up with either  $^3\text{He}$  or  $\text{BF}_3$ . The electrons produced by the secondary ionization interact with the positively charged anode wire. One disadvantage of this detector is that it cannot be attained a desired thickness since it is very difficult to have a fixed thickness with a gas. In contrast, in scintillator detectors since detection is developed in a solid, any thickness can be obtained. The thinner the thickness of the solid the more efficient the results obtained become. Usually the absorber is  $^6\text{Li}$  and the substrate, which detects the products, is phosphor, which exhibits luminescence. This emission of light produced from the phosphor results from the excitation of this when the ions pass thorough the scintillator. Then the signal produced is collected and transduced to an electrical signal in order to tell that a neutron has been detected.

#### 6.4.4 Neutron scattering

One of the greatest features of neutron scattering is that neutrons are scattered by every single atomic nucleus in the material whereas in X-ray studies, these are scattered by the electron density. In addition, neutron can be scattered by the magnetic moment of the atoms. The intensity of the scattered neutrons will be due to the wavelength at which it is executed from the source. Figure 6.93 shows how a neutron is scattered by the target when the incident beam hits it.

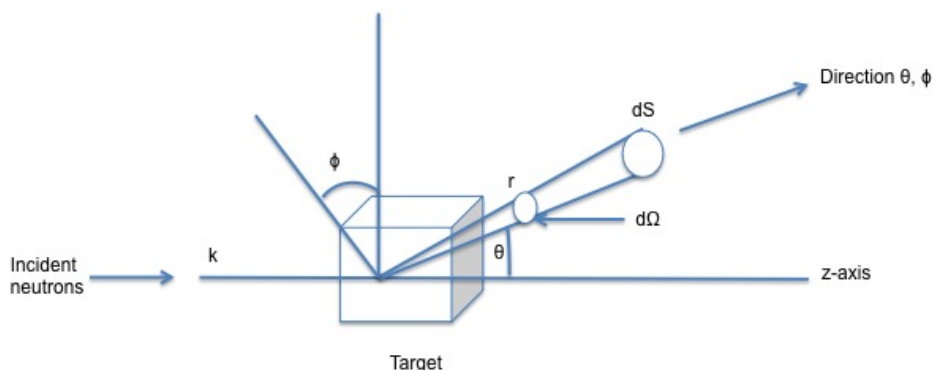


**Figure 6.93:** Schematic representation of scattering of neutrons when it hits the target. Adapted from W. Marshall and S. W. Lovesey, *Theory of thermal neutron scattering: the use of neutrons for the investigation of condensed matter*, Clarendon Press, Oxford (1971).

The incident beam encounters the target and the scattered wave produced from the collision is detected by a detector at a defined position given by the angles  $\theta$ ,  $\phi$  which are joined by the  $d\Omega$ . In this scenario there is assumed that there is no transferred energy between the nucleus of the atoms and the neutron ejected, leads to an elastic scattering.

When there is an interest in calculating the diffracted intensities the cross sectional area needs to be separated into scattering and absorption respectively. In relation to the energies of these there is moderately large range for constant scattering cross section. Also, there is a wide range cross sections close to the nuclear resonance. When the energies applied are less than the resonance the scattering length and scattering cross

section are moved to the negative side depending on the structure being examined. This means that there is a shift on the scattering, therefore the scattering will not be in a  $180^\circ$  phase. When the energies are higher than resonance it means that the cross section will be asymptotic to the nucleus area. This will be expected for spherical structures. There is also resonance scattering when there are different isotopes because each produce different nuclear energy levels.

#### 6.4.4.1 Coherent and incoherent scattering

Usually in every material, atoms will be arranged differently. Therefore, neutrons when scattered will be either coherently or incoherently. It is convenient to determine the differential scattering cross section, which is given by (6.18), where  $b$  represents the mean scattering length of the atoms,  $k$  is the scattering vector,  $r_n$  is the position of the vector of the analyzed atom and lastly  $N$  is the total number of atoms in the structure. This equation can be separated in two parts, which one corresponds to the coherent scattering and the incoherent scattering as labeled below. Usually the particles scattered will be coherent which facilitates the solution of the cross section but when there is a difference in the mean scattering length, there will be a complete arrangement of the formula and these new changes (incoherent scattering) should be considered. Incoherent scattering is usually due to the isotopes and nuclear spins of the atoms in the structure.

$$d\sigma/d\Omega = \underbrace{|b|^2 |\sum \exp(ik \cdot r_n)|^2}_{\text{coherent}} + \underbrace{N|b-b|^2}_{\text{incoherent}} \quad (6.18)$$

The ability to distinguish atoms with similar atomic number or isotopes is proportional to the square of their corresponding scattering lengths. There are already known several coherent scattering lengths of some atoms which are very similar to each other. Therefore, it makes even easier to identify by neutrons the structure of a sample. Also neutrons can find ions of light elements because they can locate very low atomic number elements such as hydrogen. Due to the negative scattering that hydrogen develops it increases the contrast leading to a better identification of it, although it has a very large incoherent scattering which causes electrons to be removed from the incident beam applied.

#### 6.4.4.2 Magnetic scattering

As previously mentioned one of the greatest features about neutron diffraction is that neutrons because of their magnetic moment can interact with either the orbital or the spin magnetic moment of the material examined. Not all every single element in the periodic table can exhibit a magnetic moment. The only elements that show a magnetic moment are those, which have unpaired electrons spins. When neutrons hit the solid this produces a scattering from the magnetic moment vector as well as the scattering vector from the neutron itself. Below Figure 6.94 shows the different vectors produced when the incident beam hits the solid.

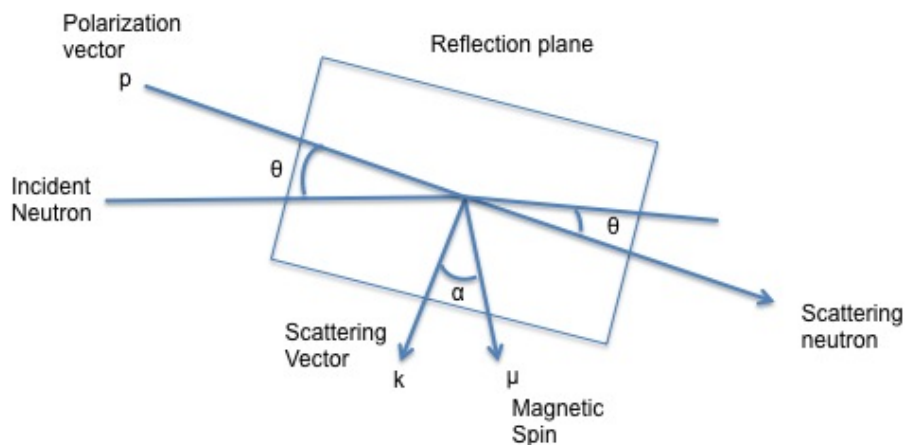


**Figure 6.94:** Diagram of magnetic Scattering of neutrons. Adapted from G. E. Bacon, *Neutron Diffraction*, Clarendon Press, Oxford (1975).

When looking at magnetic scattering it needs to be considered the coherent magnetic diffraction peaks where the magnetic contribution to the differential cross section is  $p^2q^2$  for an unpolarized incident beam. Therefore the magnetic structure amplitude will be given by (6.18), where  $q_n$  is the magnetic interaction vector,  $p_n$  is the magnetic scattering length and the rest of the terms are used to know the position of the atoms in the unit cell. When this term  $F_{\text{mag}}$  is squared, the result is the intensity of magnetic contribution from the peak analyzed. This equation only applies to those elements which have atoms that develop a magnetic moment.

$$F_{\text{mag}} = \sum p_n q_n \exp\{2\pi i(hx_n + ky_n + lz_n)\}$$

Magnetic diffraction becomes very important due to its d-spacing dependence. Due to the greater effect produced from the electrons in magnetic scattering the forward scattering has a greater strength than the backward scattering. There can also be developed similar as in X-ray, interference between the atoms which makes structure factor also be considered. These interference effects could be produced by the wide range in difference between the electron distribution and the wavelength of the thermal neutrons. This factor quickly decreases as compared to X-rays because the beam only interacts with the outer electrons of the atoms.

### 6.4.5 Sample preparation and environment

In neutron diffraction there is not a unique protocol of factors that should be considered such as temperature, electric field and pressure to name a few. Depending on the type of material and data that has been looked the parameters are assigned. There can be reached very high temperatures such as 1800K or it can go as low as 4K. Usually to get to these extreme temperatures a special furnace capable of reaching these temperatures needs to be used. For example, one of the most common used is the He refrigerator when working with very low temperatures. For high temperatures, there are used furnaces with a heating element cylinder such as vanadium (V), niobium (Nb), tantalum (Ta) or tungsten (W) that is attached to copper bars which hold the sample. Figure 6.95 shows the design for the vacuum furnaces used for the analysis. The metal that works best at the desired temperature range will be the one chosen as the heating element. The metal that is commonly used is vanadium because it prevents the contribution of other factors such as coherent scattering. Although with this metal this type of scattering is almost completely reduced. Other important factor about this furnaces is that the material been examined should not decompose under vacuum conditions. The

crystal needs to be as stable as possible when it is being analyzed. When samples are not able to persist at a vacuum environment, they are heated in the presence of several gases such as nitrogen or argon.

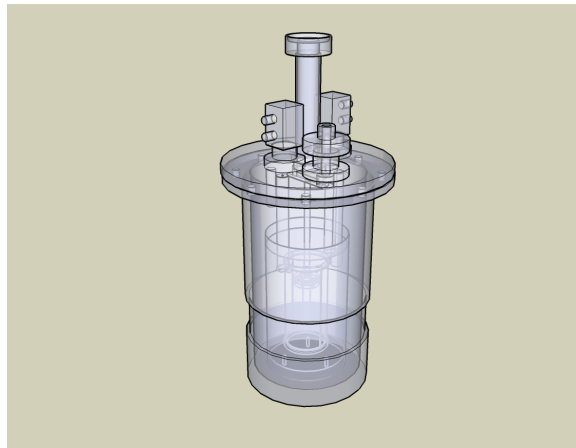


**Figure 6.95:** Metallic chamber which holds the sample. Courtesy of Nuclear Physics Institute.

Usually in order to prepare the samples that are being examined in neutron diffraction it is needed large crystals rather small ones as the one needed for X-ray studies. This one of the main disadvantages of this instrument. Most experiments are carried out using a four-circle diffractometer. The main reason being is because several experiment are carried out using very low temperatures and in order to achieve a good spectra it is needed the He refrigerator. First, the crystal being analyzed is mounted on a quartz slide, which needs to be a couple millimeters in size. Then, it is inserted into the sample holder, which is chosen depending on the temperatures wanted to be reached. In addition, neutrons can also analyze powder samples and in order to prepare the sample for these they need to be completely rendered into very fine powders and then inserted into the quartz slide similarly to the crystal structures. The main concern with this method is that when samples are grounded into powders the structure of the sample being examined can be altered.

#### 6.4.6 Summary

Neutron diffraction is a great technique used for complete characterization of molecules involving light elements and also very useful for the ones that have different isotopes in the structure. Due to the fact that neutrons interact with the nucleus of the atoms rather than with the outer electrons of the atoms such as X-rays, it leads to a more reliable data. In addition, due to the magnetic properties of the neutrons there can be characterized magnetic compounds due to the magnetic moment that neutrons develop. There are several disadvantages as well, one of the most critical is that there needs to be a good amount of sample in order to be analyzed by this technique. Also, great amounts of energy are needed to produce large amounts of neutrons. There are several powerful neutron sources that have been developed in order to conduct studies of largest molecules and a smaller quantity of sample. However, there is still the need of devices which can produce a great amount of flux to analyze more sophisticated samples. Neutron diffraction has been widely studied due to the fact that it works together with X-rays studies for the characterization of crystalline samples. The properties and advantages of this technique can greatly increased if some of the disadvantages are solved. For example, the study of molecules which exhibit some type of molecular force can be characterized. This will be because neutrons can precisely locate hydrogen atoms in a sample. Neutrons have gives a better

answer to the chemical interactions that are present in every single molecule, whereas X-rays help to give an idea of the macromolecular structure of the samples being examined.

### 6.4.7 Bibliography

- G. E. Bacon, *Neutron Diffraction*, Clarendon Press, Oxford (1975).
- R. K. Crawford, *SPIE*, 1992, **1737**, 210.
- B. D. Cullity, *Elements of X-Ray Diffraction*, 3<sup>rd</sup> Edition, Prentice Hall, New Jersey (2001).
- W. Marshall and S. W. Lovesey, *Theory of thermal neutron scattering: the use of neutrons for the investigation of condensed matter*, Clarendon Press, Oxford (1971).
- D. P. Mitchel and P. N. Powers, *Phys. Rev.*, 1936, **50**, 486.
- C. G. Shull and E. O. Wollan, *Phys. Rev.*, 1951, **81**, 527.

## 6.5 XAFS

### 6.5.1 XAFS Analysis for Arsenic Adsorption onto Iron Oxides<sup>14</sup>

#### 6.5.1.1 Introduction

X-ray absorption fine structure (XAFS) spectroscopy includes both X-ray absorption near edge structure (XANES) and extended X-ray absorption fine structure (EXAFS) spectroscopies. The difference between both techniques is the area to analyze, as shown Figure 6.96 and the information each technique provides. The complete XAFS spectrum is collected across an energy range of around 200 eV before the absorption edge of interest and until 1000 eV after it (Figure 6.96). The absorption edge is defined as the X-ray energy when the absorption coefficient has a pronounced increasing. This energy is equal to the energy required to excite an electron to an unoccupied orbital.

---

<sup>14</sup>This content is available online at <<http://cnx.org/content/m38287/1.2/>>.

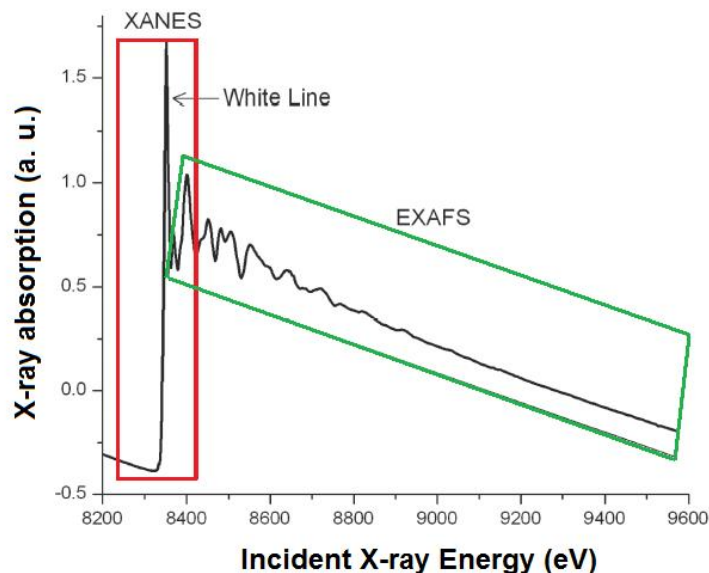


**Figure 6.96:** Characteristic spectra areas for X-ray absorption near edge structure (XANES) and extended X-ray absorption fine structure (EXAFS) spectroscopies. Adapted from S. D. Kelly, D. Hesterberg, and B. Ravel in *Methods of Soil Analysis: Part 5, Mineralogical Methods*, Ed. A. L. Urely and R. Drees, Soil Science Society of America Book Series, Madison (2008).

X-ray absorption near edge structure (XANES) is used to determine the valence state and coordination geometry, whereas extended X-ray absorption fine structure (EXAFS) is used to determine the local molecular structure of a particular element in a sample.

#### 6.5.1.1.1 X-ray absorption near edge structure (XANES) spectra

XANES is the part of the absorption spectrum closer an absorption edge. It covers from approximately -50 eV to +200 eV relative to the edge energy (Figure 6.96). Because the shape of the absorption edge is related to the density of states available for the excitation of the photoelectron, the binding geometry and the oxidation state of the atom affect the XANES part of the absorption spectrum.

Before the absorption edge, there is a linear and smooth area. Then, the edge appears as a step, which can have other extra shapes as isolated peaks, shoulders or a *white line*, which is a strong peak onto the edge. Those shapes give some information about the atom. For example, the presence of a white line indicates that after the electron releasing, the atomic states of the element is confined by the potential it feels. This peak sharp would be smoothed if the atom could enter to any kind of resonance. Important information is given because of the absorption edge position. Atoms with higher oxidation state have fewer electrons than protons, so, the energy states of the remaining electrons are lowered slightly, which causes a shift of the absorption edge energy up to several eV to a higher X-ray energy.

#### 6.5.1.1.2 Extended X-ray absorption fine structure (EXAFS) spectra

The EXAFS part of the spectrum is the oscillatory part of the absorption coefficient above around 1000 eV of the absorption edge. This region is used to determine the molecular bonding environments of the elements. EXAFS gives information about the types and numbers of atoms in coordination a specific atom and their

inter-atomic distances. The atoms at the same radial distance from a determinate atom form a shell. The number of the atoms in the shell is the coordination number (e.g., Figure 6.97).

---

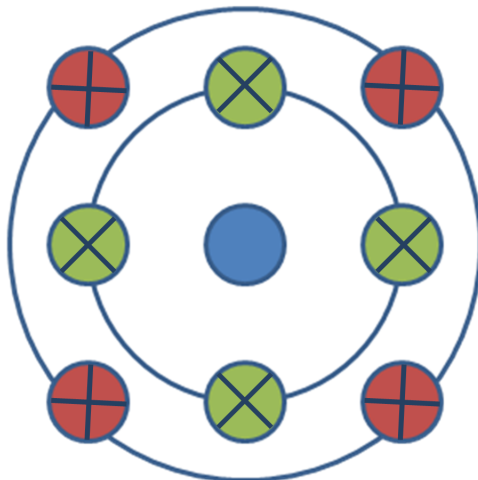


**Figure 6.97:** A schematic representation of coordination number in different layers in which there are two shells around the center atom. Both shells, green (x) and red (+), have coordination numbers of 4, but the radial distance of the red one (+) is bigger than the green one (x). Based on S. D. Kelly, D. Hesterberg, and B. Ravel in *Methods of Soil Analysis: Part 5, Mineralogical Methods*, Ed. A. L. Urely and R. Drees, Soil Science Society of America Book Series, Madison (2008).

---

An EXAFS signal is given by the photoelectron scattering generated for the center atom. The phase of the signal is determinate by the distance and the path the photoelectrons travel. A simple scheme of the different paths is shown by Figure 6.98. In the case of two shells around the centered atom, there is a degeneracy of four for the path between the main atom to the first shell, a degeneracy of four for the path between the main atom to the second shell, and a degeneracy of eight for the path between the main atom to the first shell, to the second one and to the center atom.

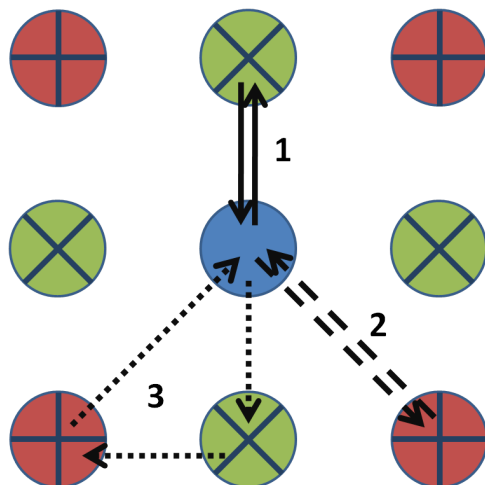


**Figure 6.98:** A two shell diagram in which there are three kinds of paths. From the center atom to the green one (x) and then going back (1); from the center atom to the red one (+) and the going back (2); and from the center atom to the first shell to the second one, and the returning to the center atom (3). Based on S. D. Kelly, D. Hesterberg, and B. Ravel in *Methods of Soil Analysis: Part 5, Mineralogical Methods*, Ed. A. L. Urely and R. Drees, Soil Science Society of America Book Series, Madison (2008).

The analysis of EXAFS spectra is accomplished using Fourier transformation to fit the data to the EXAFS equation. The EXAFS equation is a sum of the contribution from all scattering paths of the photoelectrons (6.19), where each path is given by (6.20).

$$\chi(k) = \sum_i \chi_i(k) \quad (6.19)$$

$$\chi_i(k) \equiv \frac{(N_i S_0^2) F_{\text{eff}i}(k)}{k R_i^2} \sin[2kR_i + \phi_i(k)] e^{-2\sigma_i^2 k^2} e^{-\frac{2R_i}{\lambda(k)}} \quad (6.20)$$

The terms  $F_{\text{eff}i}(k)$ ,  $\phi_i(k)$ , and  $\lambda_i(k)$  are the effective scattering amplitude of the photoelectron, the phase shift of the photoelectron, and the mean free path of the photoelectron, respectively. The term  $R_i$  is the half path length of the photoelectron (the distance between the centered atom and a coordinating atom for a single-scattering event). And the  $k^2$  is given by the (6.21). The remaining variables are frequently determined by modeling the EXAFS spectrum.

$$k^2 = \frac{2m_e(E - E_0 + \Delta E_0)}{\hbar} \quad (6.21)$$

### 6.5.1.2 XAFS analysis for arsenic adsorption onto iron oxides

The absorption of arsenic species onto iron oxide offers an example of the information that can be obtained by EXAFS. Because of the huge impact that the presence of arsenic in water can produce in societies there is a lot of research in the adsorption of arsenic in several kinds of materials, in particular nano materials. Some of the materials more promising for this kind of applications are iron oxides. The elucidation of the

mechanism of arsenic coordination onto the surfaces of those materials has been studied lately using X-ray absorption spectroscopy.

There are several ways how arsenate ( $\text{AsO}_4^{3-}$ , Figure 6.99) can be adsorbed onto the surfaces. Figure 6.100 shows the three ways that Sherman proposes arsenate can be adsorbed onto goethite ( $\alpha\text{-FeOOH}$ ): bidentate cornersharing (2C), bidentate edge sharing (2E) and monodentate corner-sharing (1V) shapes. Figure 6.101 shows that the bidentate corner sharing (2C) is the configuration that corresponds with the calculated parameters not only for goethite, but for several iron oxides.

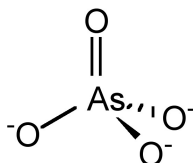


**Figure 6.99:** Structure of the arsenate anion.

---

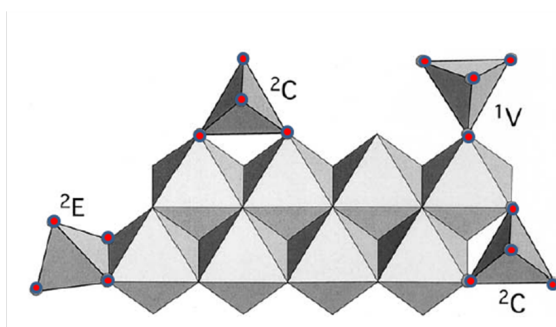


**Figure 6.100:** Possible configurations of arsenate onto goethite. The tetrahedral with the small spheres represents the arsenate ions. Adapted from D. M. Sherman and S. R. Randal. *Geochim. Cosmochim. Ac.* 2003, **67**, 4223.

---

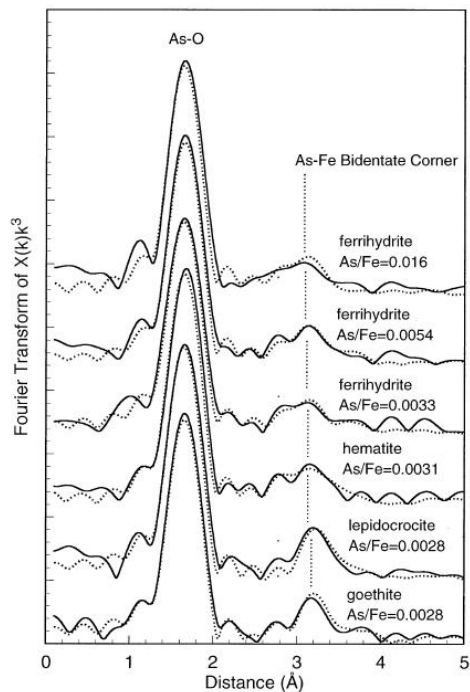


**Figure 6.101:** Fourier transforms of the EXAFS for arsenate sorbed onto goethite, lepidocrocite, hematite and ferrihydrite. Adapted from D. M. Sherman and S. R. Randal. *Geochim. Cosmochim. Ac.* 2003, **67**, 4223.

Several studies have confirmed that the bidentate corner sharing (2C) is the one present in the arsenate adsorption but also one similar, a tridentate corner sharing complex (3C), for the arsenite adsorption onto most of iron oxides as shows Figure 6.102. Table 6.11 shows the coordination numbers and distances reported in the literature for the As(III) and As(V) onto goethite.

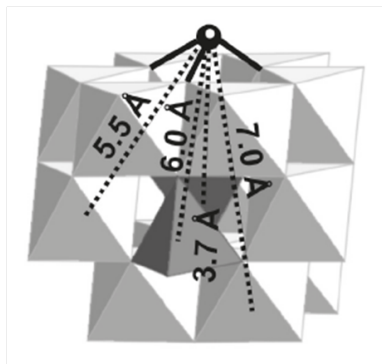


**Figure 6.102:** Proposed structural model for arsenic(III) tridante. Adapted from G. Morin, Y. Wang, G. Ona-Nguema, F. Juillot, G. Calas, N. Menguy, E. Aubry, J. R. Bargar, and G. E. Brown. *Langmuir* 2009, **25**, 9119.

As	CN As-O	R As-O ( Å )	CN As-Fe	R As-Fe ( Å )
III	3.06±0.03	1.79±0.8	2.57±0.01	3.34±3
	3.19	1.77±1	1.4	3.34±5
	3	1.78	2	3.55±5
V	1.03.0	1.631.70	2	3.30
	4.6	1.68	–	3.55±5

**Table 6.11:** Coordination numbers (CN) and inter-atomic distances (R) reported in the literature for the As(III) and As(V) adsorption onto goethite.

### 6.5.1.3 Bibliography

- G. Bunker. *Introduction to XAFS: A practical guide to X-ray Absorption Fine Structure Spectroscopy*, Cambridge University Press, Cambridge (2010).
- S. D. Kelly, D. Hesterberg, and B. Ravel in *Methods of Soil Analysis: Part 5, Mineralogical Methods*, Ed. A. L. Urely and R. Drees, Soil Science Society of America Book Series, Madison (2008).
- G. A. Waychunas, B. A. Rea, C. C. Fuller, and J. A. Davis. *Geochim. Cosmochim. Ac.* 1993, **57**, 2251.
- B. A. Manning, and S. E. Fendorf, and S. Goldberg, *Environ. Sci. Techn.*, 1998, **32**, 2383.
- D. M. Sherman and S. R. Randal, *Geochim. Cosmochim. Ac.*, 2003, **67**, 4223.
- G. Ona-Nguena, G. Morin F. Juillot, G. Calas, and G. E. Brown, *Environ. Sci. Techn.*, 2005, **39**, 9147.
- M. Stachowicz, T. Hiemstra, and W. H. Van Riemsdijk, *J. Colloid. Interf. Sci.*, 2005, **302**, 62.
- M. Auffan, J. Rose, O. Proux, D. Borschneck, A. Masion, P. Chaurand, J. L. Hazemann, C. Chaneac, J. P. Jolivet, M. R. Wiesner, A. Van Geen, and J. Y. Bottero, *Langmuir*, 2008, **24**, 3215.
- G. Ona-Nguena, G. Morin, Y. Wang, N. Menguy, F. Juillot, L. Olivi, G. Aquilanti, M. Abdelmoula, C. Ruby, J. R. Bargar, F. Guyot, G. Calas, and G. E. Brown, Jr., *Geochim. Cosmochim. Ac.*, 2009, **73**, 1359.

- G. Morin, Y. Wang, G. Ona-Nguema, F. Juillot, G. Calas, N. Menguy, E. Aubry, J. R. Bargar, and G. E. Brown Jr., *Langmuir*, 2009, **25**, 9119.
- J. Rose, M. M. Cortalezzi-Fidalgo, S. Moustier, C. Magonetto, C. D. Jones, A. R. Barron, M. R. Wiesner, and J.-Y. Bottero, *Chem. Mater.*, 2002, **14**, 621.

## 6.6 Circular Dichroism Spectroscopy and its Application for Determination of Secondary Structure of Optically Active Species<sup>15</sup>

### 6.6.1 Introduction

Circular dichroism (CD) spectroscopy is one of few structure assessment methods that can be utilized as an alternative and amplification to many conventional analysis techniques with advantages such as rapid data collection and ease of use. Since most of the efforts and time spent in advancement of chemical sciences are devoted to elucidation and analysis of structure and composition of synthesized molecules or isolated natural products rather than their preparation, one should be aware of all the relevant techniques available and know which instrument can be employed as an alternative to any other technique.

The aim of this module is to introduce CD technique and discuss what kind of information one can collect using CD. Additionally, the advantages of CD compared to other analysis techniques and its limitations will be shown.

#### 6.6.1.1 Optical activity

As CD spectroscopy can analyze only optically active species, it is convenient to start the module with a brief introduction of optical activity. In nature almost every life form is handed, meaning that there is a certain degree of asymmetry, just like in our hands. One cannot superimpose right hand on the left because they are non-identical mirror images of one another. So are the chiral (handed) molecules, they exist as enantiomers, which are mirror images of each other (Figure 6.103). One interesting phenomenon related to chiral molecules is their ability to rotate the plane of polarized light. Optical activity property is used to determine specific rotation,  $[\alpha]_{\lambda}^T$ , of a pure enantiomer. This feature is used in polarimetry to find the *enantiomeric excess*, (ee), present in a sample.

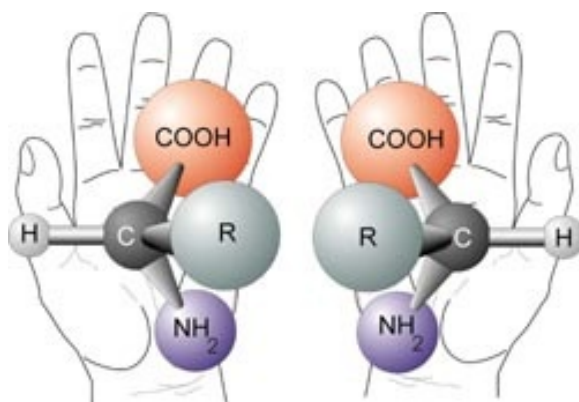


**Figure 6.103:** Schematic depiction of chirality/handedness of an amino acid.

<sup>15</sup>This content is available online at <<http://cnx.org/content/m38277/1.2/>>.

### 6.6.1.2 Circular dichroism

Circular dichroism (CD) spectroscopy is a powerful yet straightforward technique for examining different aspects of optically active organic and inorganic molecules. Circular dichroism has applications in variety of modern research fields ranging from biochemistry to inorganic chemistry. Such widespread use of the technique arises from its essential property of providing structural information that cannot be acquired by other means. One other laudable feature of CD is its being a quick, easy technique that makes analysis a matter of minutes. Nevertheless, just like all methods, CD has a number of limitations, which will be discussed while comparing CD to other analysis techniques.

CD spectroscopy and related techniques were considered as esoteric analysis techniques needed and accessible only to a small clandestine group of professionals. In order to make the reader more familiar with the technique, first of all, the principle of operation of CD and its several types, as well as related techniques will be shown. Afterwards, sample preparation and instrument use will be covered for protein secondary structure study case.

Depending on the light source used for generation of circularly polarized light, there are:

- Far UV CD, used to study secondary structure proteins.
- Near UV CD, used to investigate tertiary structure of proteins.
- Visible CD, used for monitoring metal ion protein interactions.

### 6.6.1.3 Principle of operation

In the CD spectrometer the sample is placed in a cuvette and a beam of light is passed through the sample. The light (in the present context all electromagnetic waves will be referred to as light) coming from source is subjected to circular polarization, meaning that its plane of polarization is made to rotate either clockwise (right circular polarization) or anti-clockwise (left circular polarization) with time while propagating, see Figure 6.104.

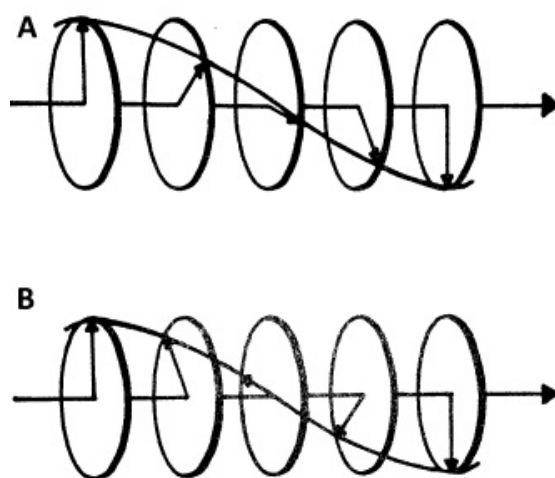


**Figure 6.104:** Schematic representation of (a) right circularly polarized and (b) left circularly polarized light. Adapted from L. Que, *Physical Methods in Bioinorganic Chemistry – Spectroscopy and Magnetism*, University Science Books, Sausalito (2000).

The sample is, firstly irradiated with left rotating polarized light, and the absorption is determined by (6.22). A second irradiation is performed with right polarized light. Now, due to the intrinsic asymmetry of chiral molecules, they will interact with circularly polarized light differently according to the direction of rotation there is going to be a tendency to absorb more for one of rotation directions. The difference between absorption of left and right circularly polarized light is the data, which is obtained from (6.23), where  $\epsilon_L$  and  $\epsilon_R$  are the molar extinction coefficients for left and right circularly polarized light,  $c$  is the molar concentration,  $l$  is the path length, the cuvette width (in cm). The difference in absorption can be related to difference in extinction,  $\Delta\epsilon$ , by (6.24).

$$A = \epsilon c l \quad (6.22)$$

$$\Delta A = A_L - A_R = (\epsilon_L - \epsilon_R) c l \quad (6.23)$$

$$\Delta\epsilon = \epsilon_L - \epsilon_R \quad (6.24)$$

Usually, due to historical reasons the CD is reported not only as difference in absorption or extinction coefficients but as degree of ellipticity,  $[\theta]$ . The relationship between  $[\theta]$  and  $\Delta\epsilon$  is given by (6.25).

$$[\theta] = 3,298 \Delta\epsilon \quad (6.25)$$

Since the absorption is monitored in a range of wavelengths, the output is a plot of  $[\theta]$  versus wavelength or  $\Delta\epsilon$  versus wavelength. Figure 6.105 shows the CD spectrum of  $\Delta$ -[Co(en)<sub>3</sub>]Cl<sub>3</sub>.

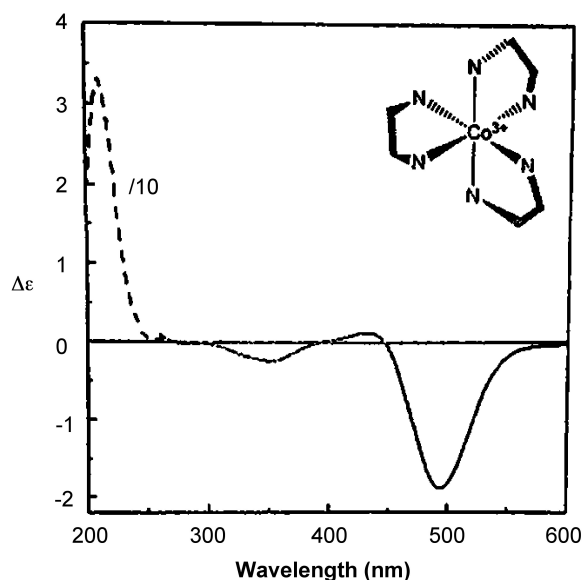


**Figure 6.105:** CD spectrum of  $\Delta$ -[Co(en)<sub>3</sub>]Cl<sub>3</sub>.

## 6.6.2 Related techniques

### 6.6.2.1 Magnetic circular dichroism

Magnetic circular dichroism (MCD) is a sister technique to CD, but there are several distinctions:

- MCD does not require the sample to possess intrinsic asymmetry (i.e., chirality/optical activity), because optical activity is induced by applying magnetic field parallel to light.
- MCD and CD have different selection rules, thus information obtained from these two sister techniques is different. CD is good for assessing environment of the samples' absorbing part while MCD is superior for obtaining detailed information about electronic structure of absorbing part.

MCD is powerful method for studying magnetic properties of materials and has recently been employed for analysis of iron-nitrogen compound, the strongest magnet known. Moreover, MCD and its variation, variable temperature MCD are complementary techniques to Mossbauer spectroscopy and electron paramagnetic resonance (EPR) spectroscopy. Hence, these techniques can give useful amplification to the chapter about Mossbauer and EPR spectroscopy.

### 6.6.2.2 Linear dichroism

Linear dichroism (LD) is also a very closely related technique to CD in which the difference between absorbance of perpendicularly and parallelly polarized light is measured. In this technique the plane of polarization of light does not rotate. LD is used to determine the orientation of absorbing parts in space.

## 6.6.3 Advantages and limitations of CD

Just like any other instrument CD has its strengths and limits. The comparison between CD and NMR shown in Table 6.12 gives a good sense of capabilities of CD.

CD	NMR
Molecules of any size can be studied	There is size limitation
The experiments are quick to perform; single wavelength measurements require milliseconds.	This is not the case all of the time.
Unique sensitivity to asymmetry in sample's structure.	Special conditions are required to differentiate between enantiomers.
Can work with very small concentrations, by lengthening the cuvette width until discernable absorption is achieved.	There is a limit to sensitivity of instrument.
Timescale is much shorter (UV) thus allowing to study dynamic systems and kinetics.	Timescale is long, use of radio waves gives average of all dynamic systems.
Only qualitative analysis of data is possible.	Quantitative data analysis can be performed to estimate chemical composition.
<i>continued on next page</i>	

Does not provide atomic level structure analysis	Very powerful for atomic level analysis, providing essential information about chemical bonds in system.
The observed spectrum is not enough for claiming one and only possible structure	The NMR spectrum is key information for assigning a unique structure.

**Table 6.12:** A comparison of CD spectroscopy to NMR spectroscopy.

#### 6.6.4 What kind of data is obtained from CD?

One effective way to demonstrate capabilities of CD spectroscopy is to cover the protein secondary structure study case, since CD spectroscopy is well-established technique for elucidation of secondary structure of proteins as well as any other macromolecules. By using CD one can estimate the degree of conformational order (what percent of the sample proteins is in  $\alpha$ -helix and/or  $\beta$ -sheet conformation), see Figure 6.106.

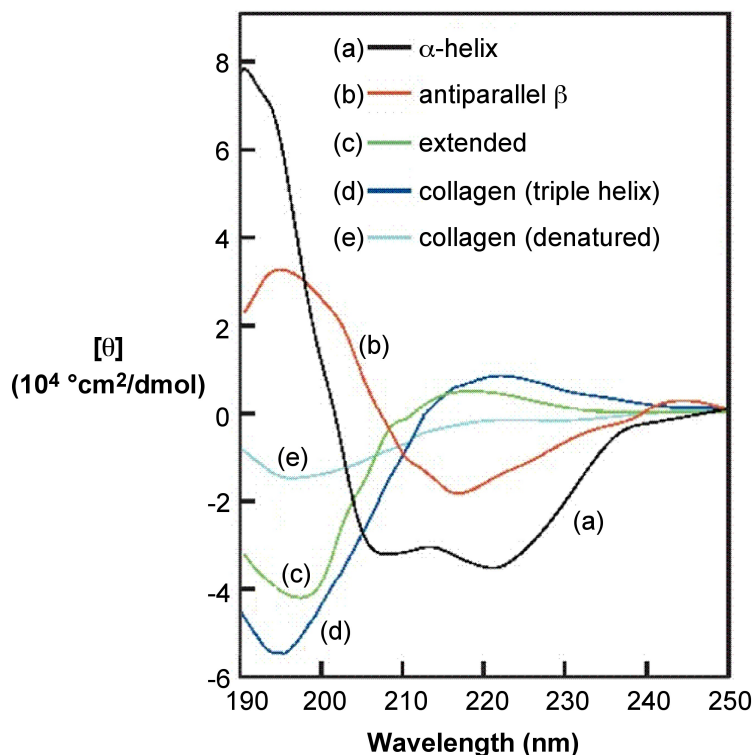


**Figure 6.106:** CD spectra of samples with representative conformations. Adapted by permission from N. Greenfield, *Nat. Proto.*, 2006, **1**, 6.

Key points for visual estimation of secondary structure by looking at a CD spectrum:

- $\alpha$ -helical proteins have negative bands at 222 nm and 208 nm and a positive band at 193 nm.
- $\beta$ -helices have negative bands at 218 nm and positive bands at 195 nm.

- Proteins lacking any ordered secondary structure will not have any peaks above 210 nm.

Since the CD spectra of proteins uniquely represent their conformation, CD can be used to monitor structural changes (due to complex formation, folding/unfolding, denaturation because of rise in temperature, denaturants, change in amino acid sequence/mutation, etc. ) in dynamic systems and to study kinetics of protein. In other words CD can be used to perform stability investigations and interaction modeling.

### 6.6.5 CD instrument

Figure 6.107 shows a typical CD instrument.

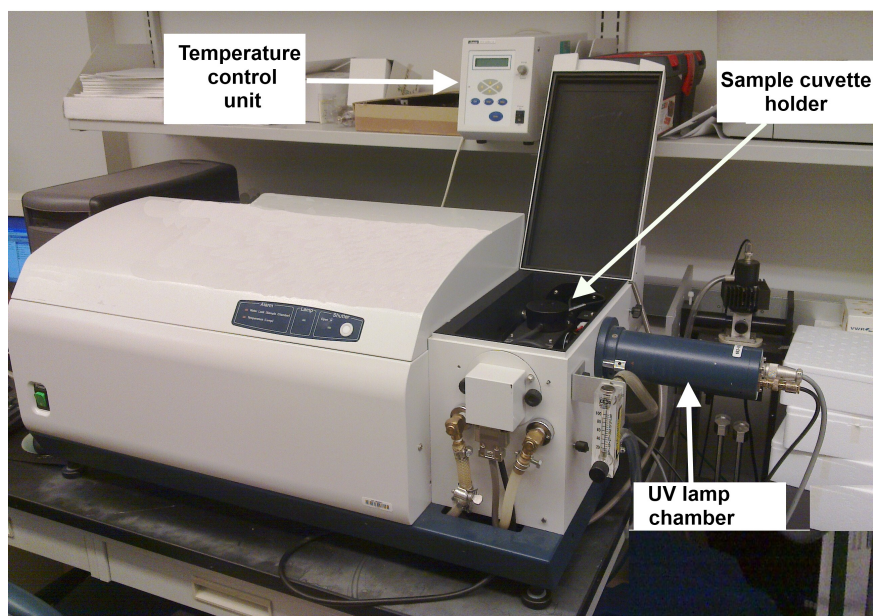


Figure 6.107: A CD instrument.

### 6.6.6 Protocol for collecting a CD spectrum

Described is a general procedure for data collection, options (time constant of instrument, wavelength interval, half-bandwidth) can be varied according to needs through the instrument controlling program.

#### 6.6.6.1 Sample preparation and starting the instrument

Most of proteins and peptides will require using buffers in order to prevent denaturation. Caution should be shown to avoid using any optically active buffers. Clear solutions are required. CD is taken in high transparency quartz cuvettes to ensure least interference. There are cuvettes available that have path-length ranging from 0.01 cm to 1 cm. Depending on UV activity of buffers used one should choose a cuvette with path-length (distance the beam of light passes through the sample) that compensates for UV absorbance of buffer. Solutions should be prepared according to cuvette that will be used, see Table 6.13.

Cuvette path (cm)	Concentration of sample (mg/mL)
0.01 - 0.02	0.2 – 1.0
0.1	0.05 – 0.2
1	0.005 – 0.01

**Table 6.13:** Choosing the appropriate cuvette based upon the sample concentration.

Besides, just like salts used to prepare pellets in FT-IR, the buffers in CD will show cutoffs at a certain point in low wavelength region, meaning that buffers start to absorb after certain wavelength. The cutoff values for most of common buffers are known and can be found from manufacturer. Oxygen absorbs light below 200 nm. Therefore, in order to remove interference buffers should be prepared from distilled water or the water should be degassed before use. Another important point is to accurately determine concentration of sample, because concentration should be known for CD data analysis. Concentration of sample can be determined from extinction coefficients, if such are reported in literature also for protein samples quantitative amino acid analysis can be used.

Many CD instrument come bundled with a sample compartment temperature control unit. This is very handy when doing stability and unfolding/denaturation studies of proteins. Check to make sure the heat sink is filled with water. Turn the temperature control unit on and set to chosen temperature.

UV source in CD is very powerful lamp and can generate large amounts of Ozone in its chamber. Ozone significantly reduces the life of the lamp. Therefore, oxygen should be removed before turning on the main lamp (otherwise it will be converted to ozone near lamp). For this purpose nitrogen gas is constantly flushed into lamp compartment. Let Nitrogen flush at least for 15 min. before turning on the lamp.

### 6.6.6.2 Collecting spectra for blank, water, buffer background, and sample

- Step 1. Collect spectrum of air blank (Figure 6.108). This will be essentially a line lying on x-axis of spectrum, zero absorbance.
- Step 2. Fill the cuvette with water and take a spectrum.
- Step 3. Water droplets left in cuvette may change concentration of your sample, especially when working with dilute samples. Hence, it is important to thoroughly dry the cuvette. After drying the cuvette, collect spectrum of buffer of exactly same concentration as used for sample (Figure 6.108). This is the step where buffer is confirmed to be suitable spectrum of the buffer and water should overlap within experimental error, except for low wavelength region where signal-to-noise ratio is low.
- Step 4. Clean the cuvette as described above and fill with sample solution. Collect the CD spectrum for three times for better accuracy (Figure 6.108). For proteins multiple scans should overlap and not drift with time.

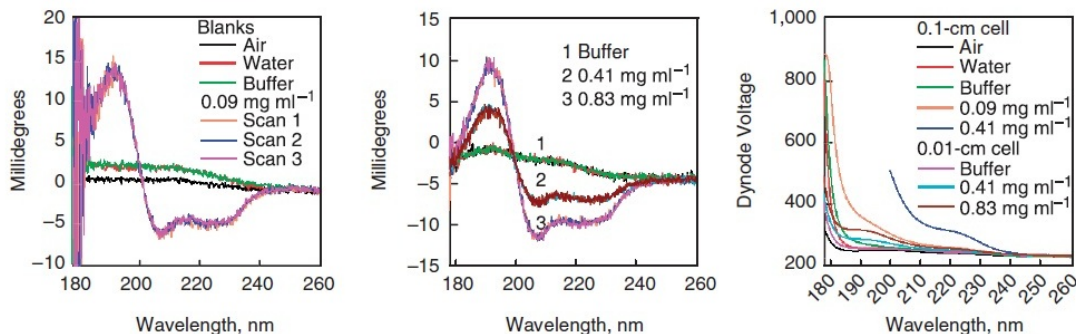


**Figure 6.108:** CD spectra of blank and water (left), buffer (center), and sample (right). Lysozyme in 10 mM sodium phosphate pH 7. Adapted by permission from N. Greenfield, *Nat. Protoc.*, 2006, **1**, 6.

### 6.6.6.3 Data handling and analysis

After saving the data for both the spectra of the sample and blank is smoothed using built-in commands of controller software. The smoothed baseline is subtracted from the smoothed spectrum of the sample. The next step is to use software bundles which have algorithms for estimating secondary structure of proteins. Input the data into the software package of choice and process it. The output from algorithms will be the percentage of a particular secondary structure conformation in sample. The data shown in Figure 6.109 lists commonly used methods and compares them for several proteins. The estimated secondary structure is compared to X-ray data, and one can see that it is best to use several methods for best accuracy.

METHOD		X-Ray	LINCOMB	MLR	CONTIN	SELCON	VARSLC	K2D	CDNN						
Lowest wavelength, nm		200	178	200	178	200	190	200	178	200	178	200	200	180	
Myoglobin	$\alpha$ -helix	78	96	93	89	97	67	89	73	79	76	74	74	83	84
	$\beta$ -sheet	0	0	0	0	0	0	0	-3	0	0	0	8	3	2
	Turn	10	4	5	8	3	16	0	13	20	4	18	ND	9	9
Lactate dehydrogenase	$\alpha$ -helix	37	46	40	63	42	46	40	41	39	40	39	55	42	44
	$\beta$ -sheet	14	21	29	15	33	7	39	12	27	15	28	11	13	10
	Turn	25	15	11	13	9	26	1	22	27	17	13		15	14
Chymotrypsin	$\alpha$ -helix	10	15	21	33	28	11	9	7	15	24	16	12	19	20
	$\beta$ -sheet	38	25	14	6	0	16	32	16	26	0	11	33	29	50
	Turn	26	10	16	5	9	44	32	13	16	42	39	ND	21	22
Bence Jones protein	$\alpha$ -helix	3	0	0	0	0	6	0	3	9	14	0	3	13	16
	$\beta$ -sheet	50	43	40	68	40	42	81	47	34	7	69	50	39	22
	Turn	24	25	29	17	28	25	10	23	40	28	17	ND	22	22
Lowest wavelength, nm		200	190	200	190	200	190	200	178	200	178	200	200	180	
Poly(lys-leu)n	$\alpha$ -helix	0	0	9	0	2	12	9	31	24	31	30	5	34	39
	$\beta$ -sheet	100	89	65	89	99	73	91	24	39	51	55	89	18	13
	Turn	0	11	26	7	0	0	0	26	26	1	3	ND	16	13
Lowest wavelength, nm		200	190	200	190	200	190	200	190	200	190	200	190	190	
Poly-L-lysine 0.01% helical form, pH 11.1	$\alpha$ -helix	100	97	100	-	-	100	100	99	89	100	96	100	92	94
	$\beta$ -sheet	0	3	0	-	-	0	0	0	1	6	18	0	1	1
	Turn	0	0	0	-	-	0	0	1	6	13	15	0	7	7

**Figure 6.109:** Comparison of secondary structure estimation methods. Adapted by permission from N. Greenfield, *Nat. Protoc.*, 2006, **1**, 6.

### 6.6.7 Conclusion

What advantages CD has over other analysis methods? CD spectroscopy is an excellent, rapid method for assessing the secondary structure of proteins and performing studies of dynamic systems like folding and binding of proteins. It worth noting that CD does not provide information about the position of those subunits with specific conformation. However, CD outrivals other techniques in rapid assessing of the structure of unknown protein samples and in monitoring structural changes of known proteins caused by ligation and complex formation, temperature change, mutations, denaturants. CD is also widely used to juxtapose fused proteins with wild type counterparts, because CD spectra can tell whether the fused protein retained the structure of wild type or underwent changes.

### 6.6.8 Bibliography

- L. Que, *Physical Methods in Bioinorganic Chemistry – Spectroscopy and Magnetism*, University Science Books, Sausalito (2000).
- J. P. Wang, J. Nian, L. Xiaoqi, X. Yunhao, and C. S. Hanke, *New J. Phys.*, 2010, **12**, 063032.
- N. Greenfield, *Nat. Protoc.*, 2006, **1**, 6.
- G. Holzwarth and P. Doty, *J. Am. Chem. Soc.*, 1965, **87**, 218.
- N. Greenfield and G.D. Fasman, *Biochemistry*, 1969, **8**, 4108.
- P. Atkins and J. de Paula, *Elements of Physical Chemistry*, 4th ed, Oxford University Press (2005).
- M. Rutherford and M. Dunn, *Curr. Protoc. Protein Sci.*, 2011, **63**, 3.2.1.

## 6.7 Protein Analysis using Electrospray Ionization Mass Spectroscopy<sup>16</sup>

### 6.7.1 Introduction

Electrospray ionization-mass spectrometry (ESI-MS) is an analytical method that focuses on macromolecular structural determination. The unique component of ESI-MS is the electrospray ionization. The development of electrospraying, the process of charging a liquid into a fine aerosol, was completed in the 1960's when Malcolm Dole (Figure 6.110) demonstrated the ability of chemical species to be separated through electrospray techniques. With this important turn of events, the combination of ESI and MS was feasible and was later developed by John B. Fenn (Figure 6.111), as a functional analytical method that could provide beneficial information about the structure and size of a protein. Fenn shared the Nobel Prize in 2002, with Koichi Tanaka (Figure 6.112) and Kurt Wüthrich (Figure 6.113) for the development of ESI-MS.

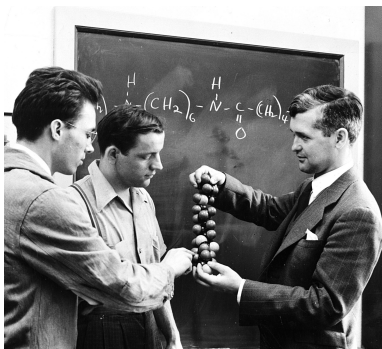


**Figure 6.110:** American chemist Malcolm Dole (on right) (1903 – 1990).

---

<sup>16</sup>This content is available online at <<http://cnx.org/content/m38341/1.1/>>.



**Figure 6.111:** American chemist John Bennett Fenn (1917 - 2010) shared the Nobel Prize for his work in ESI-MS and other identification and structural analyses of biological molecules.

---



**Figure 6.112:** Japanese chemist and Nobel laureate Tanaka (1959 - ).

---

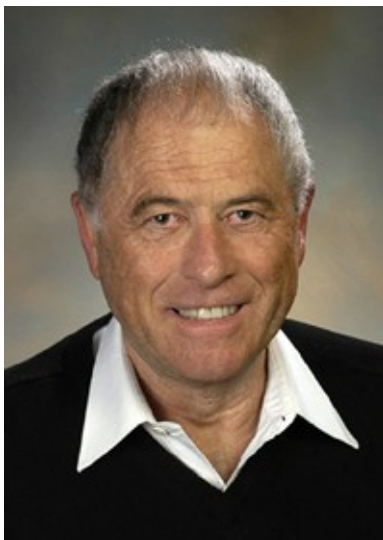


**Figure 6.113:** Swiss chemist and Nobel laureate Kurt Wüthrich (1938 – ).

---

ESI-MS is the process through which proteins, or macromolecules, in the liquid phase are charged and fragmented into smaller aerosol droplets. These aerosol droplets lose their solvent and propel the charged fragments into the gas phase in several components that vary by charge. These components can then be detected by a mass spectrometer. The recent boom and development of ESI-MS is attributed to its benefits in characterizing and analyzing macromolecules, specifically biologically important macromolecules such as proteins.

### 6.7.2 How does ESI-MS function?

ESI-MS is a process that requires the sample to be in liquid solution, so that tiny droplets may be ionized and analyzed individually by a mass spectrometer. The following delineates the processes that occur as relevant to Figure 6.114:

- **Spray needle/capillary-** The liquid solution of the desired macromolecule is introduced into the system through this needle. The needle is highly charged via an outside voltage source that maintains the charge constant across the needle. The normal charge for a needle is approximately 2.5 to 4 kV. The voltage causes the large droplets to fragment into small droplets based on charge that is accumulated from the protein constituent parts, and the liquid is now in the gas phase.
- **Droplet formation-** The droplets that are expelled from the needle are smaller than initially, and as a result the solvent will evaporate. The smaller droplets then start increasing their charge density on the surface as the volume decreases. As the droplets near the Rayleigh limit, Coulombic interactions of the droplet equal the surface tension of the droplet, a *Coulombic explosion* occurs that further breaks the droplet into minute fractions, including the isolated analyte with charge.
- **Vacuum interface/cone -** This portion of the device allows for the droplets to align in a small trail and pass through to the mass spectrometer. Alignment occurs because of the similarity and differences in charges amongst all the droplets. All the droplets are ionized to positive charges through addition of protons to varying basic sites on the droplets, yet all the charges vary in magnitude dependent upon

the number of basic sites available for protonation. The receiving end or the cone has the opposite charge of the spray needle, causing an attraction between the cone and the droplets.

- Mass spectrometer- The charged particles then reach the mass spectrometer and are deflected based on the charge of each particle. Deflection occurs by the quadrupole magnet of the mass spectrometer. The different deflection paths of the ions occur due to the strength of the interaction with the magnetic field. This leads to various paths based on a mass/charge ( $m/z$ ) ratio. The particles are then read by the ion detector, as they arrive, providing a spectrum based on  $m/z$  ratio.

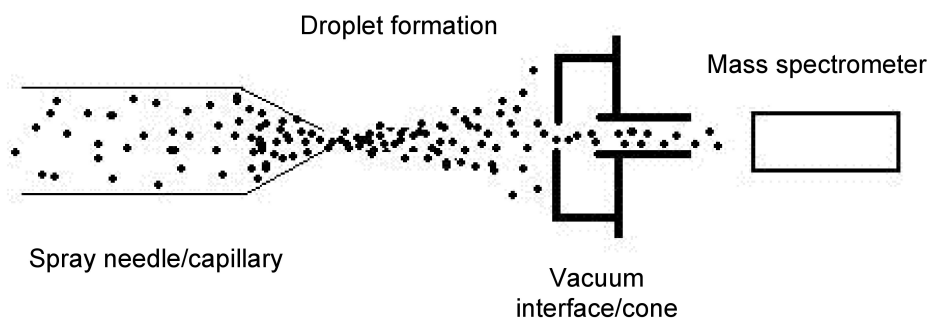


**Figure 6.114:** The process of ESI-MS. A focus on the capillary spray needle and the generation of aerosol particles.

---

### 6.7.3 What data is provided by ESI-MS?

As implied by the name, the data produced from this technique is a mass spectrometry spectrum. Without delving too deeply into the topic of mass spectrometry, which is out of the true scope of this module, a slight explanation will be provided here. The mass spectrometer separates particles based on a magnetic field created by a quadrupole magnet. The strength of the interaction varies on the charge the particles carry. The amount of deflection or strength of interaction is determined by the ion detector and quantified into a mass/charge ( $m/z$ ) ratio. Because of this information, determination of chemical composition or peptide structure can easily be managed as is explained in greater detail in the following section.

### 6.7.4 Interpretation of a typical MS spectrum

Interpreting the mass spectrometry data involves understanding the  $m/z$  ratio. The knowledge necessary to understanding the interpretation of the spectrum is that the peaks correspond to portions of the whole molecule. That is to say, hypothetically, if you put a human body in the mass spectrometer, one peak would coincide with one arm, another peak would coincide with the arm and the abdomen, etc. The general idea behind these peaks, is that an overlay would paint the entire picture, or in the case of the hypothetical example, provide the image of the human body. The  $m/z$  ratio defines these portions based on the charges carried by them; thus the terminology of the mass/charge ratio. The more charges a portion of the macromolecule or protein holds, the smaller the  $m/z$  ratio will be and the farther left it will appear on the spectrum. The fundamental concept behind interpretation involves understanding that the peaks are interrelated, and thus the math calculations may be carried out to provide relevant information of the protein or macromolecule being analyzed.

### 6.7.5 Calculation of $m/z$ of the MS spectrum peaks

As mentioned above, the pertinent information to be obtained from the ESI-MS data is extrapolated from the understanding that the peaks are interrelated. The steps for calculating the data are as follow:

- Step 1. Determine which two neighboring peaks will be analyzed.
- Step 2. Establish the first peak (the one farthest left) as the peak with the greatest  $m/z$  ratio. This is mathematically defined as our  $z+1$  peak.
- Step 3. Establish the adjacent peak to the right of our first peak as the peak with the lower  $m/z$  ratio. This is mathematically our  $z$  peak.
- Step 4. Our  $z+1$  peak will also be our  $m+1$  peak as the difference between the two peaks is the charge of one proton. Consequently, our  $z$  peak will be defined as our  $m$  peak.
- Step 5. Solve both equations for  $m$  to allow for substitution. Both sides of the equation should be in terms of  $z$  and can be solved.
- Step 6. Determine the charge of the  $z$  peak and subsequently, the charge of the  $z+1$  peak.
- Step 7. Subtract one from the  $m/z$  ratio and multiply the  $m/z$  ratio of each peak by the previous charges determined to obtain the mass of the protein or macromolecule.
- Step 8. Average the results to determine the average mass of the macromolecule or protein.

#### Example 6.2

- Step 1. Determine which two neighboring peaks will be analyzed from the MS (Figure 6.115) as the  $m/z = 5$  and  $m/z = 10$  peaks.

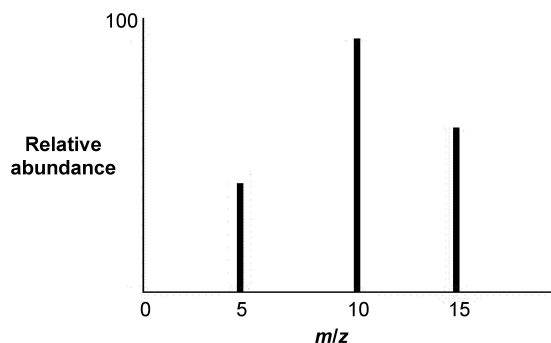


**Figure 6.115:** Hypothetical mass spectrometry data; not based off of any particular compound. The example steps are based off of this spectrum.

- Step 2. Establish the first peak (the one farthest left in Figure 6.115) as the  $z + 1$  peak (i.e.,  $z + 1 = 5$ ).
- Step 3. Establish the adjacent peak to the right of the first peak as the  $z$  peak (i.e.,  $z = 10$ ).
- Step 4. Establish the peak ratios, (6.26) and (6.27).

$$\frac{m+1}{z+1} = 5 \tag{6.26}$$

$$\frac{m}{z} = 10 \tag{6.27}$$

Step 5. Solve the ratios for  $m$ : (6.28) and (6.29).

$$m = 5z + 4 \tag{6.28}$$

$$m = 10z \tag{6.29}$$

Step 6. Substitute one equation for  $m$ : (6.30).

$$5z + 4 = 10z \tag{6.30}$$

Step 7. Solve for  $z$ : (6.31).

$$z = 4/5 \tag{6.31}$$

Step 8. Find  $z + 1$ : (6.32).

$$z + 1 = 9/5 \tag{6.32}$$

Step 9. Find average molecular mass by subtracting the mass by 1 and multiplying by the charge: (6.33) and (6.34). Hence, the average mass = 7.2.

$$(10 - 1)(4/5) = 7.2 \tag{6.33}$$

$$(5 - 1)(9/5) = 7.2 \tag{6.34}$$

### 6.7.6 Sample preparation

Samples for ESI-MS must be in a liquid state. This requirement provides the necessary medium to easily charge the macromolecules or proteins into a fine aerosol state that can be easily fragmented to provide the desired outcomes. The benefit to this technique is that solid proteins that were once difficult to analyze, like metallothionein, can dissolved in an appropriate solvent that will allow analysis through ESI-MS. Because the sample is being delivered into the system as a liquid, the capillary can easily charge the solution to begin fragmentation of the protein into smaller fractions. Maximum charge of the capillary is approximately 4 kV. However, this amount of charge is not necessary for every macromolecule. The appropriate charge is dependent on the size and characteristic of the solvent and each individual macromolecule. This has allowed for the removal of the molecular weight limit that was once held true for simple mass spectrometry analysis of proteins. Large proteins and macromolecules can now easily be detected and analyzed through ESI-MS due to the facility with which the molecules can fragment.

### 6.7.7 Related techniques

A related technique that was developed at approximately the same time as ESI-MS is matrix assisted laser desorption/ionization mass spectrometry (MALDI-MS). This technique that was developed in the late 1980's as well, serves the same fundamental purpose; allowing analysis of large macromolecules via mass spectrometry through an alternative route of generating the necessary gas phase for analysis. In MALDI-MS, a matrix, usually comprised of crystallized 3,5-dimethoxy-4-hydroxycinnamic acid (Figure 6.116), water, and an organic solvent, is used to mix the analyte, and a laser is used to charge the matrix. The matrix then co-crystallizes the analyte and pulses of the laser are then used to cause desorption of the matrix and some of the analyte crystals with it, leading to ionization of the crystals and the phase change into the gaseous state. The analytes are then read by the tandem mass spectrometer. Table 6.14 directly compares some attributes between ESI-MS and MALDI-MS. It should be noted that there are several variations of both ESI-MS and MALDI-MS, with the methods of data collection varying and the piggy-backing of several other methods (liquid chromatography, capillary electrophoresis, inductively coupled plasma mass spectrometry, etc.), yet all of them have the same fundamental principles as these basic two methods.

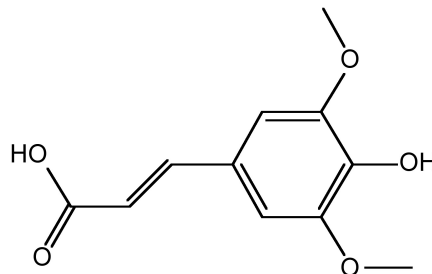


**Figure 6.116:** Structure of 3,5-dimethoxy-4-hydroxycinnamic acid.

Experimental details	ESI-MS	MALDI-MS
Starting analyte state	Liquid	Liquid/solid
Method of ionization	Charged capillary needle	Matrix laser desorption
Final analyte state	Gas	Gas
Quantity of protein needed	1 $\mu\text{L}$	1 $\mu\text{L}$
Spectrum method	Mass spectrometry	Mass spectrometry

**Table 6.14:** Comparison of the general experimental details of ESI-MS and MALDI-MS.

### 6.7.8 Problems with ESI-MS

ESI-MS has proven to be useful in determination of tertiary structure and molecular weight calculations of large macromolecules. However, there are still several problems incorporated with the technique and macromolecule analysis. One problem is the isolation of the desired protein for analysis. If the protein is unable to be extracted from the cell, this is usually done through gel electrophoresis, there is a limiting factor in what proteins can be analyzed. Cytochrome *c* (Figure 6.117) is an example of a protein that can

be isolated and analyzed, but provides an interesting limitation on how the analytical technique does not function for a completely effective protein analysis. The problem with cytochrome *c* is that even if the protein is in its native confirmation, it can still show different charge distribution. This occurs due to the availability of basic sites for protonation that are consistently exposed to the solvent. Any slight change to the native conformation may cause basic sites, such as in cytochrome *c* to be blocked causing different  $m/z$  ratios to be seen. Another interesting limitation is seen when inorganic elements, such as in metallothioneins proteins that contain zinc, are analyzed using ESI-MS. Metallothioneins have several isoforms that show no consistent trend in ESI-MS data between the varied isoforms. The marked differences occur due to the metallation of each isoform being different, which causes the electrospraying and as a result protonation of the protein to be different. Thus, incorporation of metal atoms in proteins can have various effects on ESI-MS data due to the unexpected interactions between the metal center and the protein itself.

---

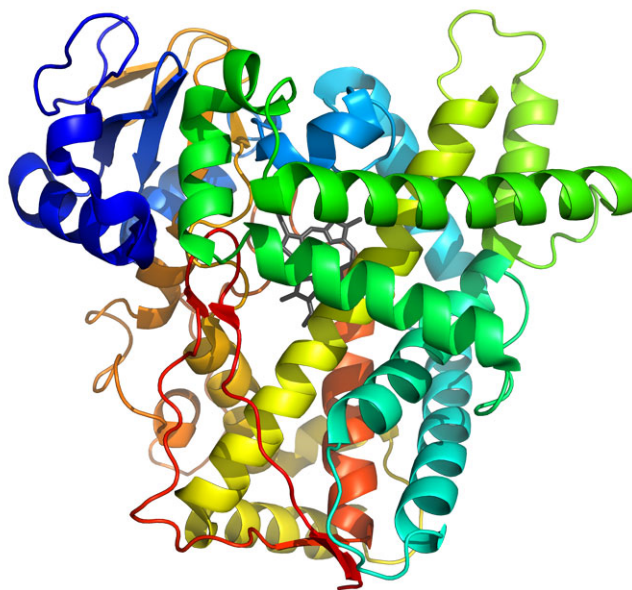


**Figure 6.117:** The 3-D structure of human cytochrome P450 2A13, a sub class of human cytochrome *c*.

---

### 6.7.9 Bibliography

- L. Konermann and D. J. Douglas, *Biochemistry*, 1997, **36**, 12296.
- S. Pérez-Rafael, S. Atrian, M. Capdevila, and Ó. Palacios, *Talanta*, 2011, **83**, 1057.
- D. L. Nelson and M. M. Cox, *Lehninger Principles of Biochemistry*, 5<sup>th</sup> Ed, W. H. Freeman and Company, New York (2008).
- A. Prange and D. Profrock, *Anal. Bioanal. Chem.*, 2005, **383**, 372.
- <http://www.chm.bris.ac.uk/ms/theory/esi-ionisation.html><sup>17</sup>

---

<sup>17</sup><http://www.chm.bris.ac.uk/ms/theory/esi-ionisation.html>



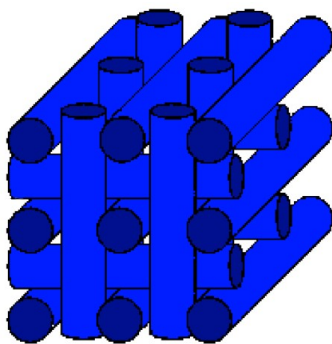


**Figure 6.119:** A schematic representation of the ordered structure of a blue LC phase.

---



**Figure 6.120:** Schematic representations of (a) a discotic nematic LC phase and (b) a discotic columnar LC phase.

---

Thermotropic LCs are very sensitive to temperature. If the temperature is too high, thermal motion will destroy the ordering of LCs, and push it into a liquid phase. If the temperature is too low, thermal motion is hard to perform, so the material will become crystal phase.

The existence of liquid crystal phase can be detected by using polarized optical microscopy, since liquid crystal phase exhibits its unique texture under microscopy. The contrasting areas in the texture correspond to domains where LCs are oriented towards different directions.

### 6.8.1.2 Polarized optical microscopy

Polarized optical microscopy is typically used to detect the existence of liquid crystal phases in a solution. The principle of this is corresponding to the polarization of light. A polarizer is a filter that only permits the light oriented in a specific direction with its polarizing direction to pass through. There are two polarizers in a polarizing optical microscope (POM) (Figure 6.121) and they are designed to be oriented at right angle to each other, which is termed as cross polar. The fundamental of cross polar is illustrated in Figure 6.122, the polarizing direction of the first polarizer is oriented vertically to the incident beam, so only the waves with vertical direction can pass through it. The passed wave is subsequently blocked by the second polarizer, since this polarizer is oriented horizontally to the incident wave.

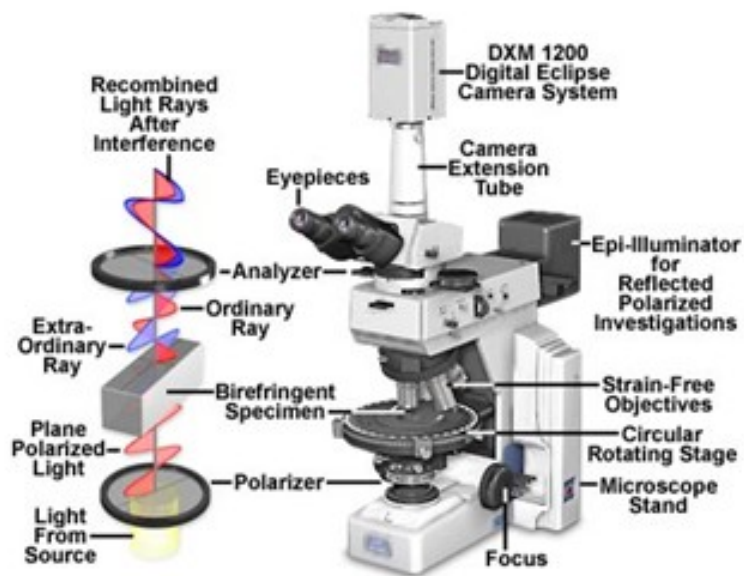


Figure 6.121: The basic configuration of polarized optical microscope. Copyright: Nikon Corporation.

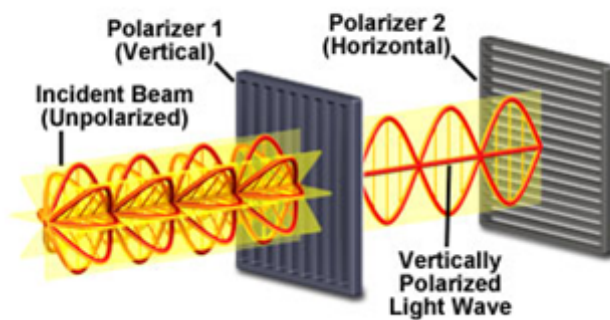
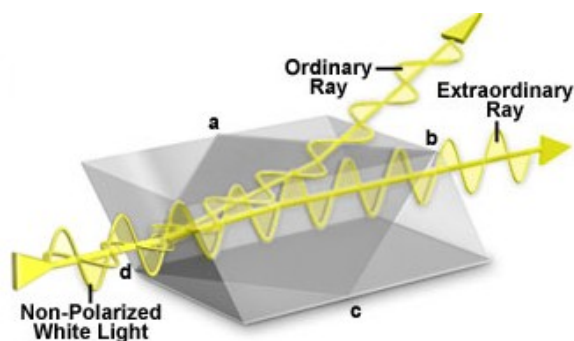


Figure 6.122: A schematic representation of the polarization of light waves. Copyright: Nikon Corporation.

### 6.8.1.3 Theory of birefringence

Birefringent or doubly-refracting sample has a unique property that it can produce two individual wave components while one wave passes through it, those two components are termed as ordinary and extraordinary waves. Figure 6.124 is an illustration of a typical construction of Nicol polarizing prism, as we can see, the non-polarized white light are splitted into two ray as it passes through the prism. The one travels out of the prism is called ordinary ray, and the other one is called extraordinary ray. So if we have a birefringent specimen located between the polarizer and analyzer, the initial light will be separated into two waves when it passes through the specimen. After exiting the specimen, the light components become out of phase, but are recombined with constructive and destructive interference when they pass through the analyzer. Now the combined wave will have elliptically or circularly polarized light wave, see Figure 6.124, image contrast arises from the interaction of plane-polarized light with a birefringent specimen so some amount of wave will pass through the analyzer and give a bright domain on the specimen.



**Figure 6.123:** A schematic representation of a Nicol polarizing prism. Copyright: Nikon Corporation.

---

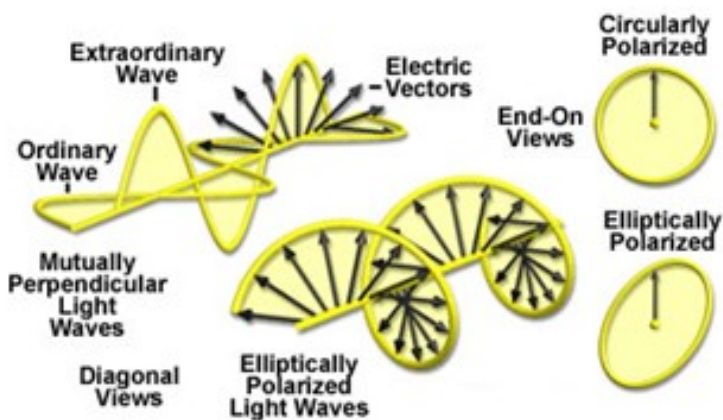


**Figure 6.124:** A schematic representation of elliptically and circularly polarized light waves. Copyright: Nikon Corporation.

#### 6.8.1.4 Liquid crystal display

The most common application of LCs are in liquid crystals displays (LCD). Figure 6.125 is a simple demonstration of how LCD works in digit calculators. There are two crossed polarizers in this system, and liquid crystal (cholesteric spiral pattern) sandwich with positive and negative charging is located between these two polarizers. When the liquid crystal is charged, waves can pass through without changing orientations. When the liquid crystal is out of charge, waves will be rotated  $90^\circ$  as it passes through LCs so it can pass through the second polarizer. There are seven separately charged electrodes in the LCD, so the LCD can exhibit different numbers from 0 to 9 by adjusting the electrodes. For example, when the upper right and lower left electrodes are charged, we can get 2 on the display.

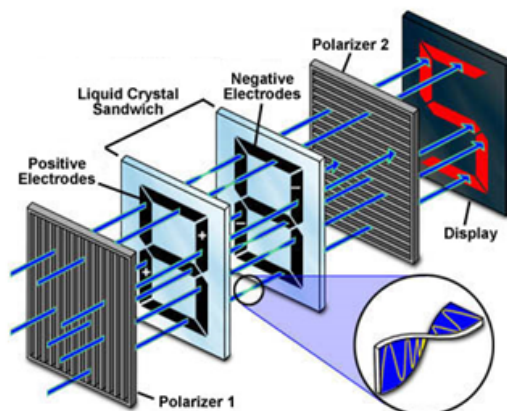


**Figure 6.125:** Demonstration of a seven-segment liquid crystal display. Copyright: Nikon Corporation.

## 6.8.2 Microscope images of liquid crystal phase

### 6.8.2.1 The first order retardation plate

The first order retardation plate is frequently utilized to determine the optical sign of a birefringent specimen in polarized light microscopy. The optical sign includes positive and negative. If the ordinary wavefront is faster than the extraordinary wavefront (see Figure 6.124), the specimen displays positive birefringence. Conversely, a negative birefringence will be detected if the ordinary wavefront is slower than the extraordinary wavefront. In addition, the retardation plate is also useful for enhancing contrast in weakly birefringent specimens. Figure 6.126 shows the effect of first order retardation plate on the contrast of birefringence. The birefringence is so weak that the morphology on the edge of the tissue is hard to image, Figure 6.126a. When a first order retardation plate is added, the structure of the cell become all apparent compared with the one without retardation plate, Figure 6.126b.

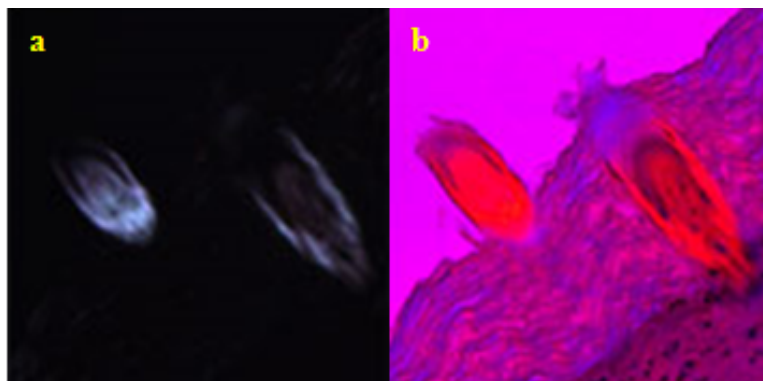


**Figure 6.126:** Microscope images of thin section of human tongue, (a) without first order retardation plate and (b) with first order retardation plate. Copyright: Olympus.

---

### 6.8.2.2 Images of liquid crystal phases

Figure 6.127 shows the images of liquid crystal phases from different specimens. First order retardation plates are utilized in all of these images. Apparent contrasts are detected here in the image which corresponds to the existence of liquid crystal phase within the specimen.

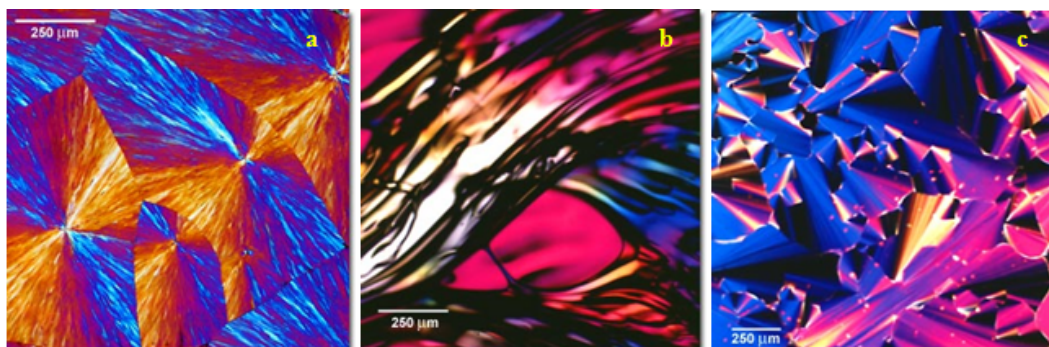


**Figure 6.127:** Microscope images in polarized light with a first-order retardation plate inserted between the specimen and analyzer: (a) polyethylene glycol, (b) polycarbonate, and (c) liquid crystalline DNA. Copyright from Nikon.

---

### 6.8.2.3 The effect of rotation of the polarizer

The effect of the angle between horizontal direction and polarizer transmission axis on the appearance of liquid crystal phase may be analyzed. In Figure 6.128 is shown images of an ascorbic acid (Figure 6.129)

sample under cross polar mode. When the polarizer rotates from  $0^\circ$  to  $90^\circ$ , big variations on the shape of bright domains and domain colors appear due to the change of wave vibrating directions. By rotating the polarizer, we can have a comprehensive understanding of the overall texture.

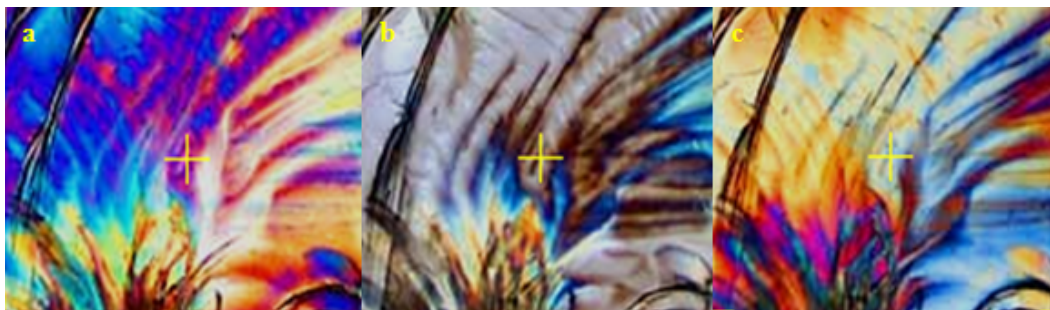


**Figure 6.128:** Cross polarized Microscope images of ascorbic acid specimen with polarizer rotation of (a)  $0^\circ$ , (b)  $45^\circ$ , and (c)  $90^\circ$ . Copyright: Nikon Corporation.

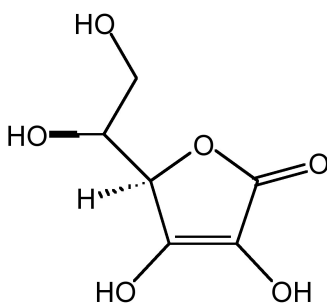


**Figure 6.129:** The structure of ascorbic acid.

### 6.8.3 Bibliography

- R. Weaver, *Am. Lab.*, 2003, **35**, 55.
- F. Massoumian, R. Juskaity, M. A. Neil, and T. Wilson, *J. Microsc.*, 2003, **209**, 13.
- R. Oldenbourg, *Nature*, 1996, **381**, 811.

## Solutions to Exercises in Chapter 6

### Solution to Exercise 6.3.2.1 (p. 515)

$2\theta$	$\theta$	$\text{Sin}\theta$	$\text{Sin}^2\theta$	$\text{Sin}^2\theta/\text{Sin}^2\theta$	$2 \times \text{Sin}^2\theta/\text{Sin}^2\theta$	$3 \times \text{Sin}^2\theta/\text{Sin}^2\theta$
38.06	19.03	0.33	0.1063	1.00	2.00	3.00
44.24	22.12	0.38	0.1418	1.33	2.67	4.00
64.35	32.17	0.53	0.2835	2.67	5.33	8.00
77.28	38.64	0.62	0.3899	3.67	7.34	11.00
81.41	40.71	0.65	0.4253	4.00	8.00	12.00
97.71	48.86	0.75	0.5671	5.33	10.67	16.00
110.29	55.15	0.82	0.6734	6.34	12.67	19.01
114.69	57.35	0.84	0.7089	6.67	13.34	20.01

**Table 6.15:** Ratio of diffraction angles for Ag.

Applying the Bragg equation (6.11),

$$1.54059 = 2d \sin 19.03$$

$$d = 2.3624 \text{ \AA}$$

Calculate the lattice parameter using (6.12),

$$1/2.3624^2 = (h^2 + k^2 + l^2)/a^2$$

$$a = 4.0918 \text{ \AA}$$

The last column gives a list of integers, which corresponds to the  $h^2+k^2+l^2$  values of the FCC lattice diffraction. Hence, the Ag nanoparticles have a FCC structure.

